VOLUME 233, 21 February 2013

ISSN 0167-2738

ELSEVIER

SOLID STATE IONICS

DIFFUSION & REACTIONS

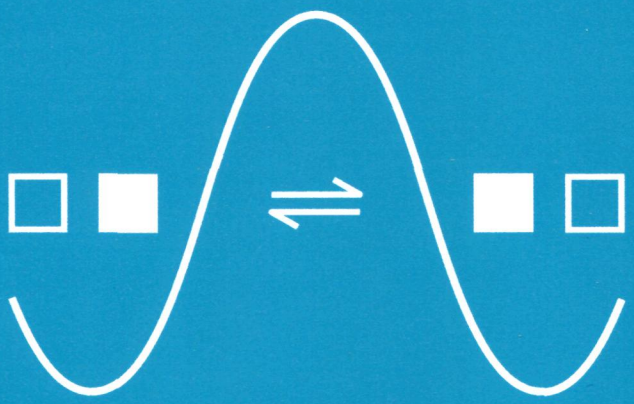

Solid State Ionics

Volume 233, Pages 1-112 (21 February 2013)

Editorial Board

High rate performance of the composites of $Li_4Ti_5O_{12}$–Ketjen Black and $Li_4Ti_5O_{12}$–Ketjen Black–multi-walled carbon nanotubes for Li-ion batteries

Highlights

► High rate performance of $Li_4Ti_5O_{12}$–KB and $Li_4Ti_5O_{12}$–KB–MWCNTs are prepared. ► KB prohibits the growth of $Li_4Ti_5O_{12}$ particles. ► MWCNTs combine with KB to form a three-dimensional conductive network. ► The asymmetric behavior between charge and discharge of $Li_4Ti_5O_{12}$ exists.

Heterovalent substitutions in $Na_2M_2TeO_6$ family: Crystal structure, fast sodium ion conduction and phase transition of $Na_2LiFeTeO_6$

Highlights

► $Na_2LiFeTeO_6$ is a new orthorhombic superlattice of the known hexagonal layered P2 type. ► The distortion seems to be only due to Na^+ ion ordering in the interlayer prisms. ► On heating, high Na^+ ion conductivity is observed, e.g., 4 S/m at 300 °C. ► With Na^+ ion movement, distortion decreases and vanishes at ca. 400 °C. ► 10 other variants of M and/or Te substitutions in $Na_2M_2TeO_6$ family were unsuccessful.

High capacity spherical $Li[Li_{0.24}Mn_{0.55}Co_{0.14}Ni_{0.07}]O_2$ cathode material for

lithium ion batteries

Original Research Article
Pages 12-19
Ying Wang, Neeraj Sharma, Dawei Su, David Bishop, Hyojun Ahn, Guoxiu Wang

Highlights

► $Li[Li_{0.24}Mn_{0.55}Co_{0.14}Ni_{0.07}]O_2$ was prepared by a modified co-precipitation method. ► The refined composition of final product is consistent with the nominal formula. ► This material exhibits high discharge capacity and satisfactory rate capability.

Effect of anode configuration on electrical properties and cell polarization in planar anode supported SOFC

Original Research Article
Pages 20-31
Madhumita Mukhopadhyay, Jayanta Mukhopadhyay, Abhijit Das Sharma, Rajendra N. Basu

Highlights

► Anodes are engineered using a novel electroless cermet having variable thickness. ► Correlation among electrical conductivity and configurational variations of anode. ► 15 μm electroless AAL augments the cell performance to 3.7 Acm^{-2} at 800 °C and 0.7 V. ► Least cell polarization (~ 0.3 $\Omega.cm^2$) is found with 15 μm electroless AAL. ► Electroless AAL substantially lowers charge transfer & concentration polarizations.

Electrode properties and microstructures of MnO_2 nanosheet thin films as cathodes for electrochemical capacitors

Original Research Article
Pages 32-37
Masato Yano, Shinya Suzuki, Masaru Miyayama, Masataka Ohgaki

Highlights

► Thin films of MnO_2 nanosheets (NS) were prepared by electrophoretic deposition. ► Small-NS films had a heterogeneous microstructure with numerous pores. ► Small-NS films exhibited better electrochemical properties than large-NS films. ► The better electrochemical properties resulted from the fast ion diffusion. ► Heterogeneous microstructure was found to contribute to the good electrode properties.

Grain boundary induced compositional stress in nanocrystalline ceria films

Original Research Article
Pages 38-46
Brian W. Sheldon, Sunil Mandowara, Janet Rankin

Highlights

► Large stresses are induced by oxidation/reduction in nanocrystalline ceria films. ► In situ experiments are consistent with space charge effects near grain boundaries. ► Measured grain boundary contributions are only a weak function of temperature.

The interface effect on the I–V curves and analysis of ionic diffusion coefficients of polycrystalline $CuIn_4Te_6$

Original Research Article
Pages 47-54
A. Arranz, R. Díaz

Highlights

► It has been found that a $CuIn_4Te_6$ polycrystal is a MIEC. ► The potential decay method is used to measure the electrical properties. ► Hysteresis effects have been observed in the I–V relations. ► An equivalent electrical circuit has been used to explain the results. ► The role of an interface residual voltage due to previous measurements is discussed.

Sulfonated poly(arylene ether sulfone)/sulfonated zeolite composite membrane for high temperature proton exchange membrane fuel cells

Original Research Article
Pages 55-61
Duk Man Yu, Young Jun Yoon, Tae-Ho Kim, Jang Yong Lee, Young Taik Hong

Highlights

► The tensile strength of the composite membrane increased from 16.52 MPa to 18.72 MPa. ► The dimensional change was reduced by approximately 40% in the composite membrane. ► Proton conductivity of the composite membrane was 1.36 times higher at 120 °C/50% RH. ► 5 wt.% sulfonated zeolite composite membrane showed a 54% increase in performance.

Energetics of lanthanum silicate apatite: Influence of interstitial oxygen and cation vacancy concentrations in $La_{9.33+x}(SiO_4)_6O_{2+3x/2}$ and

$La_{10-x}Sr_x(SiO_4)_6O_{3-0.5x}$

Original Research Article
Pages 62-66
S. Mahboobeh Hosseini, Tatiana Shvareva, Alexandra Navrotsky

Highlights

► Energetics of $La_{9.33+x}(SiO_4)_6O_{2+3x/2}$ and $La_{10-x}Sr_x(SiO_4)_6O_{3-0.5x}$ are investigated. ► Stoichiometric sample $La_8Sr_2(SiO_4)_6O_2$ is the most stable composition. ► $\Delta H°_{f,\ interstitial}$ and $\Delta H_{f,\ cation\ vacancy}$ were determined. ► Cation vacancy concentrations appear to be the dominant factor in energetics. ► Energetics in LSSO series directly correlates with conductivity.

Electrical conductivity of $La_{0.58}Sr_{0.4}Co_{0.2}Fe_{0.8}O_{3-\delta}$ during ferroelastic deformation under uniaxial compressive loading

Original Research Article
Pages 67-72
Wakako Araki, Jürgen Malzbender

Highlights

► Conductivity measurement of LSCF under uniaxial compression at various temperatures ► The enhancement in conductivity by uniaxial compressive stress is demonstrated. ► The enhancement is attributed to piezoelectric and also geometrical effects. ► The piezoelectricity of LSCF as a function of temperature up to 1073 K is obtained. ► The significant ferroelastic deformation contributes to the geometrical effect.

An interpretation for the increase of ionic conductivity by nitrogen incorporation in LiPON oxynitride glasses

Original Research Article
Pages 73-79
Nerea Mascaraque, José Luis G. Fierro, Alicia Durán, Francisco Muñoz

Highlights

► LiPON glasses with variable Li and N contents were prepared by ammonolysis. ► The lower the Li content the higher the increase of conductivity after nitridation. ► Nitrogen introduction produces a decrease of the BO/NBO ratio. ► The increase of the ionic conductivity by N depends on the variation of BO/NBO ratio.

Defect chemical modeling of Pd/ZnO Schottky junctions

Original Research Article
Pages 80-86
Shimon Saraf, Avner Rothschild

Highlights

► We present a methodology for modeling semiconducting oxide Schottky junctions. ► Our methodology accounts for the defect structure of the semiconducting oxide layer. ► The method is applied to the Pd/ZnO Schottky junction. ► The ionic defects have important role in shaping the junction characteristics. ► Growth conditions are expected to provide handles for tailoring junction properties.

A fundamental study of infiltrated CeO_2 and $(Gd,Ce)O_2$ nanoparticles on the electrocatalytic activity of Pt cathodes of solid oxide fuel cells

Original Research Article
Pages 87-94
Na Ai, Kongfa Chen, San Ping Jiang

Highlights

► Catalytic effect of infiltrated ceria and GDC NPs on Pt electrodes is investigated. ► At low currents, ceria and GDC NPs show similar promotion effect for the ORR. ► At high currents, GDC nanoparticles show higher catalytic promotion effect. ► The higher promotion effect of GDC NPs is related to its high catalytic properties.

A new crystalline LiPON electrolyte: Synthesis, properties, and electronic structure

Original Research Article
Pages 95-101
Keerthi Senevirathne, Cynthia S. Day, Michael D. Gross, Abdessadek Lachgar, N.A.W. Holzwarth

Highlights

► High temperature solid state methods were used to synthesize the new crystalline compound Li_2PO_2N. ► X-ray analysis shows the synthesized compound to have a structure similar to first-principles predictions. ► The structure is characterized by parallel chains of corner sharing

PO_2N_2 tetrahedra with planar P N P N backbones. ► Li_2PO_2N is chemically and structurally stable in air up to 600 °C and in vacuum up to 1050 °C. ► The measured Arrhenius activation energy for ionic conductivity of Li_2PO_2N in pressed pellet form is 0.6 eV.

Low temperature cubic garnet-type CO_2-doped $Li_7La_3Zr_2O_{12}$

Original Research Article
Pages 102-106
S. Toda, K. Ishiguro, Y. Shimonishi, A. Hirano, Y. Takeda, O. Yamamoto, N. Imanishi

Highlights

► Low temperature cubic phase of $Li_7La_3Zr_2O_{12}$ (LLZ) was obtained by annealing tetragonal LLZ. ► The low temperature cubic LLZ was transferred to the tetragonal phase at annealing at 800 °C for 1 h. ► The low temperature cubic LLZ contained about 2.5 wt.% CO_2.

Reply on the "critical comments on speculations with … free-volume defects … in ion-conducting Ag/AgI–As_2S_3 glasses…"

Pages 107-109
T. Kavetskyy, J. Borc, P. Petkov, K. Kolev, T. Petkova, V. Tsmots

Highlights

► Size of voids with radius R ~ 2 Å at τ_2 = 0.35–0.36 ns for g-Ag/AgI–As_2S_3 is concluded. ► This conclusion is a direct evidence of a new formula for τ_2 vs R for R < 5 Å. ► Size of voids ~ 80–100 $Å^3$ to be positron traps with τ_2 = 0.35–0.38 ns is inconclusive. ► A bias by not fixing τ_1 is small and not affecting systematic trends in PALS data.

Corrigendum

Corrigendum to "Mechanical relaxation in $(AgI)_{1-x}(Ag_2MoO_4)_x$ ionic glasses" [Solid State Ionics 113–115 (1998) 677–679]

Page 110
M. Cutroni, M. Federico, A. Mandanici, P. Mustarelli, C. Tomasi

Calendar

Page 111